Dynamic High-Torque Test Stand with Hydrostatic Drive

Dr.-Ing. Wilhelm Hagemeister*, M.Sc. Nicolai Sümnik**

Ingenieurgemeinschaft IgH GmbH, Heinz-Bäcker-Straße 34, D-45356 Essen*
E-Mail: hm@igh.de
Voith Turbo GmbH & Co. KG, Centrumstr. 2, 45307 Essen**
E-Mail: Nicolai.Suemnik@voith.com

This paper presents a Dynamic High-Torque Test Stand with hydrostatic drive technology. The topics discussed within the scope of this paper are the mechanical design and the hydraulic characteristics as well as, detailed solutions implemented in this test rig using innovative technology. The evaluation methods used to determine the test specimen properties are also described in more detail.

Keywords: elastomer coupling, test rig, hydrostatic drive, torque sensor, correlation method, ellipse identification

Target audience: test rig building, measurement technics, mechanical design

1 Introduction

Couplings with elastomer components are widely used machine elements. Their dimensioning for a given drive train is usually carried out according to DIN 740, whereby the characterizing coupling properties, stiffness and damping, are used for the design.
Couplings with high natural rubber content are subject to production fluctuations, which requires continuous testing of these properties.

Figure 1: Coupling types

The measurement of stiffness and damping is performed dynamically by way of a harmonic angular motion and measuring of the moment at a frequency of 10 Hz.

For the acceptance test of coupling elements over three torque ranges of magnitude, IgH has developed, in close cooperation with Voith Turbo, a test rig, which provides dynamic testing from 25 Nm to 50.000 Nm.

Also within the scope of this paper, other topics discussed are, the characteristic properties of the test specimens and the design and interesting technical aspects of the test bench.

2 Test Specimen

As the compensation of alignment error is usually one of the main tasks of elastomer couplings, the couplings addressed here are mainly used for torque oscillation damping and for reducing high impulse loads. One of the main operation areas is the linking of combustion engines to drive trains of e.g. mobile machinery or in railway trains driven by diesel engines.

The high rotational speed variations of a diesel engine, if coupled more or less rigid to the drive train, results in high torque levels, which can be reduced efficiently with highly flexible couplings. These couplings reduce the natural frequency, requiring more damping effects. Within the design process the selection of the right coupling for a given drive train is an important task. It especially needs to be taken into account that the resonance region must be passed quickly and also that the drive train is to be operated over-critically, meaning the minimum excitation frequency has to be above the first natural frequency of the system. Figure 2 shows an example of the frequency response of a two-mass oscillator, which is the simplified model of a drive train with a highly elastic coupling.

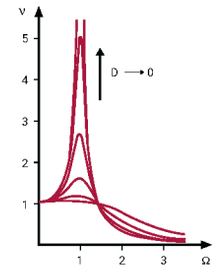

Figure 2: Frequency response of a two mass oscillator

The stiffness of the coupling - with the rotational inertia - is the dominant factor for the natural frequency of the drive train because it is usually the most flexible component. The damping is influencing the amplitude rise at the resonance frequency.

The elastomer element within the coupling is the determining factor of the entire coupling[1]. A good example would be a simple spring in parallel with a viscous damper. Stiffness and damping coefficients are of course dependent on temperature, excitation frequency and, with some materials, the amplitude of oscillation.

$$d\dot{\varphi} + C\varphi = M \tag{1}$$

W_d : dissipative work
W : reference work
M : torque
d : damping coefficient
C : dynamic stiffness
φ : angle
α, β: half axis of ellipse

[1]The coupling usually has, besides the elastomer element, also a friction damper,bearing, housing...

While deforming an elastomer element the deformation work can be split into:

- elastic energy: W, this can be reconverted into mechanical energy on the reverse movement
- viscose energy: W_d, this energy is converted into heat and then lost.

A typical torque angle characteristic curve of an elastomer element at sinusoidal torque excitation can be seen in figure: 3.

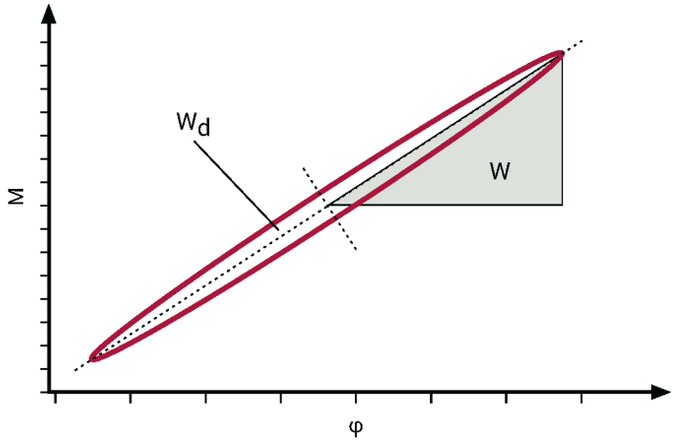

Figure 3: Torque angle characteristic of an elastomer element

W_D is the dissipative work, which can be calculated from the area of the hysteresis ellipse.

$$W_D = \pi \cdot \alpha \cdot \beta \tag{2}$$

W is the - so called - reference work, which is calculated from the surface area of the triangle which can be seen in figure 3[2].

$$W = \frac{1}{2} \cdot \varphi_{max} \cdot M\left(\varphi_{max}\right) \tag{3}$$

The characteristic material damping is defined as the quotient of the dissipative and reference work /2/.

$$\psi = \frac{W_D}{W} \tag{4}$$

The determination of the hysteresis ellipse and resulting parameters as stiffness and damping is the task of the test rig as part of the quality assurance process. Figure 4 shows a typical reading of torque and angle during a test.

During a test the coupling is loaded up to the permissible continuous alternating torque. Prior to the actual test a so called preconditioning takes place where the coupling is loaded up to the rated torque which is approximately three times the test torque. This prepares the coupling material for testing and allows its properties to stabilize. After the test the characteristic coupling parameters are calculated from the measured series of torque and angle (This is described in more detail in chapter 3.6).

[2]if the centre of the ellipse is moved in the coorinate origin

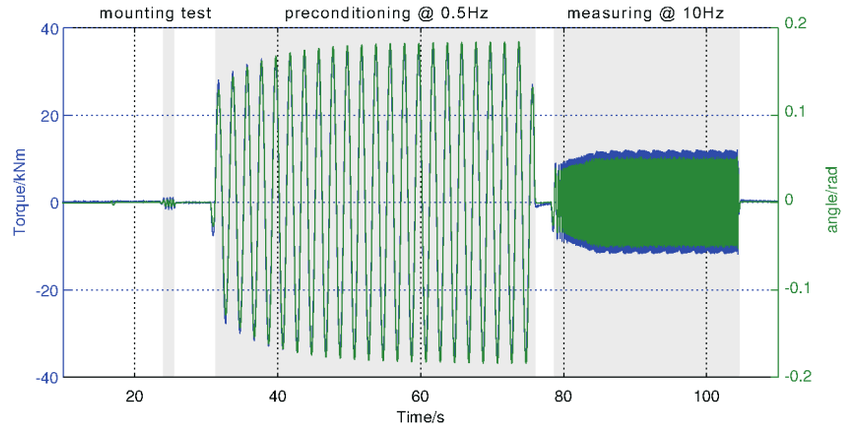

Figure 4: Time series of a acceptance test

3 Test Rig

Relevant for the design of the test rig are the parameters: torque range: 25 Nm - 50.000 Nm, a test frequency of 10 Hz with sinusoidal excitation and an angle range:[3] ±30° - ±60°. Moreover, it is required that the installation and deinstallation of the coupling should not take too much time. A low energy consumption is also desired. Besides the testing of coupling parameters, the test rig is designed to perform endurance tests, where couplings are tested at high torque rates until they fail.

3.1 Mechanical setup

As the main drive for the coupling, the principle of a hydraulic swivel motors is used.

The test specimen is mounted via the inner ring by means of an adapter without an intermediate support. This results in parasitic bending torque, axial and radial forces which act on the swivel motor bearing.

Torque is measured with a reactive sensor. The sensor is not rotating and measures the reaction torque at its support. Compared to a rotating sensor, this has the advantage that no flexible cabling needs to be guided to the sensor. Also, a compensation of rotary inertia is not necessary.

Mounting of the angle sensor is done in such a way that the deformation of the torque sensor is not relevant for the angle measurement.

Overall, this results in a compact design, which is best realized in a vertical direction. Vertically is ideal because the handling of large couplings is made easier and the customer was already equipped to handle the parts in this way.

[3]depending on coupling type

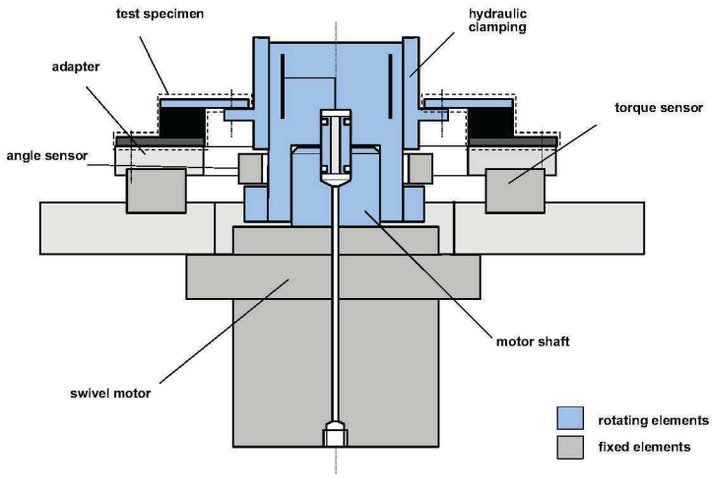

Figure 5: Concept drive train

3.2 Torque sensors

The requirement that the torque should be measured with an absolute accuracy of 1 % over the entire torque range resulted in the neccessity of having several test stations with torque sensors of different sizes. The angle range spread is a moderate $\pm 30°$ up to $\pm 60°$.

The requirement that preconditioning and measuring must be done on the same station complicates the design of the torque sensors. To realize a sensor with high sensitivity, which withstands high torque, a design with mechanical end stops was chosen.

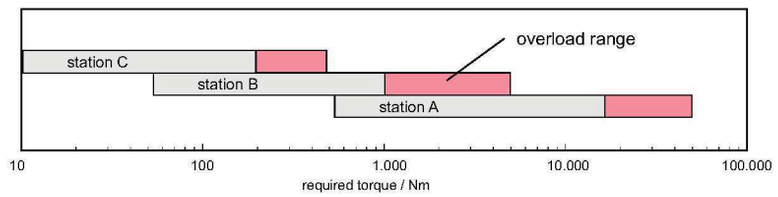

Figure 6: Torque sensor with overload range

The partitioning of the sensor ranges is shown in figure 6. The overload areas are marked in red. A torque reading in the overload range is carried out by means of calculating the torque from the hydraulic pressure difference at the swivel motor.

Figure 7 shows the design of the torque sensor with end stops for overload protection.

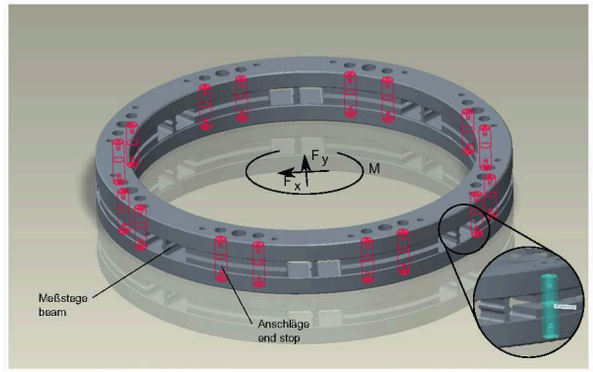

Figure 7: Torque sensor with end stops

The sensors are specially designed and are integrated optimally into the overall mechanical setup. Figure 8 shows the biggest sensor for the torque range, 500 Nm – 15.000 Nm, with an overload range up to 50.000 Nm. For torque sensing, the bending of the beams is used and the radial and axial force is measured by shear deformation. Using different deformation for torque and force allows there to be an individual influence on deformation and for an optimal design of the sensor.

Figure 8: Torque sensor for 50.000 Nm with endstops during application of the strain gauges

Figure 9 shows the functionality of the mechanical end stops. It can be seen that the end stops are reached at a torque of 24,5 kNm. For the transition between the torque signal from the sensor and the torque signal from the pressure difference of the swivel motor, a zone of 15 kNm to 16 kNm is defined.

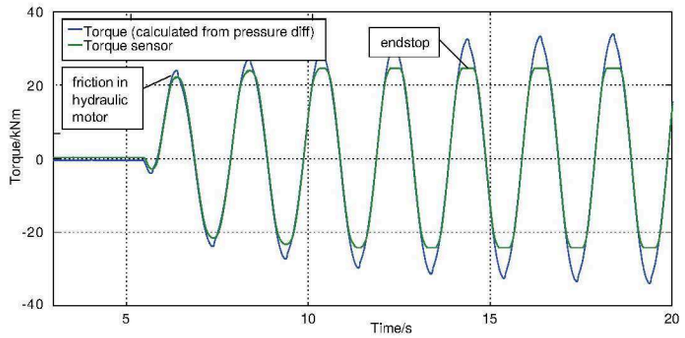

Figure 9: Functionality of the end stops

3.3 Hydraulic concept

Hydraulic swivel motors operating in the hydrostatic circuit are driven directly via a variable displacement pump[4]. A total of three different motors are used. In contrast to the otherwise usual resistance control, due to the hydrostatic transmission, in conjunction with the variable displacement volume of the hydraulic motor, the rated power usage of the test rig can be reduced to 1/4 while maintaining the same test capacity. In particular, the displacement control allows, as a matter of principle, the recovery of a portion of the work stored in the deflected clutch.

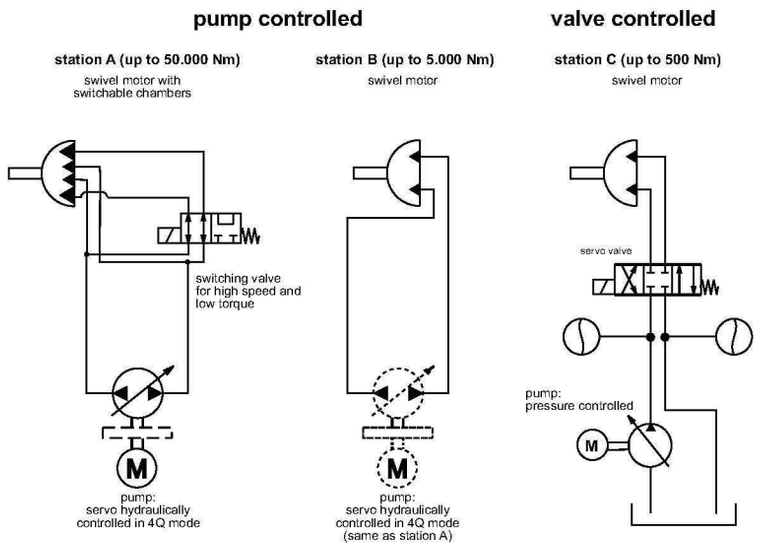

Figure 10: Hydraulic concept

As a special feature, the largest motor has a discrete variable displacement in order to be able to realize both the great moment for the preconditioning and a high adjustment speed for the measurement of the dynamic properties. The motor has three vanes, two of which can be switched off hydraulically via a switching valve. Due to the fact that the torque ratio from preconditioning to measuring is also approximately 1/3, this results in a dramatic reduction of peak supply power. The motor shaft support is realized with roller bearings to withstand high radial forces in high-speed mode. The motor was specially designed and built by the project partner Hense Systemtechnik GmbH & Co. KG who also delivered the two smaller motors.

[4]at two of the three stations

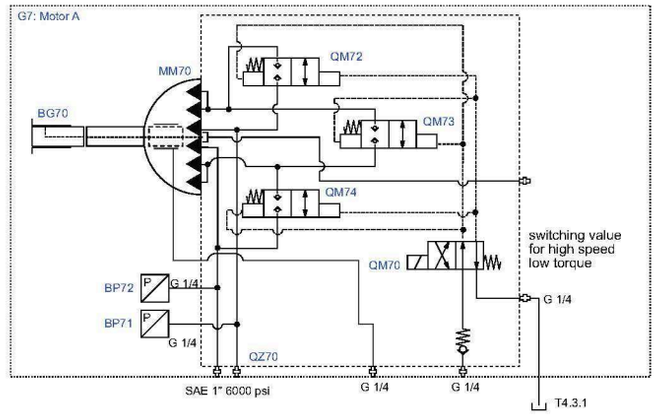

Figure 11: Swivel motor with adjustable displacement, Source: Hense

3.4 Clamping coupling

In comparison to the actual measuring time, the setup time is substantially longer. This means that for a quick coupling exchange the amount of screws needed to be reduced. For every test specimen a set of

adapters and hubs is delivered. The coupling is screwed, with help of the adapters, to the test bench and onto the hub. Torque transmission to the drive shaft is done over the hub which can be expanded hydraulically to transmit the torque via friction to the adapter. Pressure is supplied for this clamping system via a central hole in the motor shaft. Max clamping pressure is 700 bar. Figure 13 shows the setup for two different coupling types and a cross-sectional view of the clamping system.

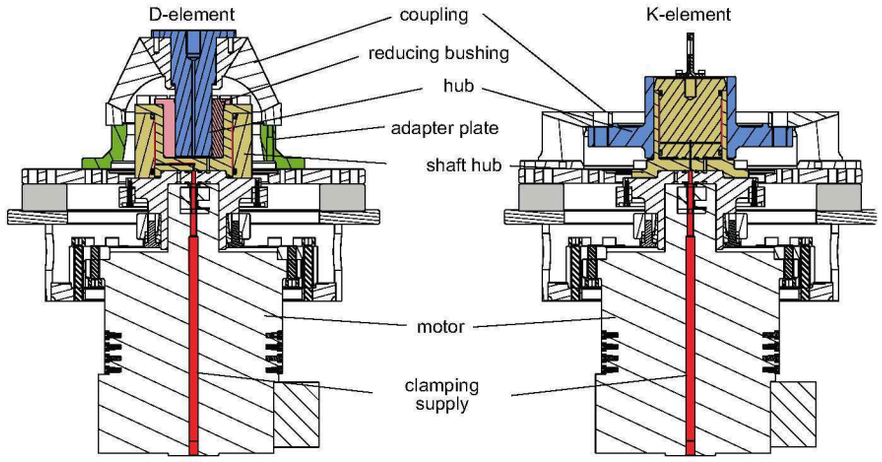

Figure 12: Cross-sectional view of the clamping system

The clamping system was designed according to Barlow's formula for thin-walled components with a comparative FEM calculation for two load cases to confirm the accuracy of the assumption. The design of the clamping system is an optimization problem with the parameters: wall thickness, clamping length, tolerances and required clamping pressure for a given torque and material parameters.

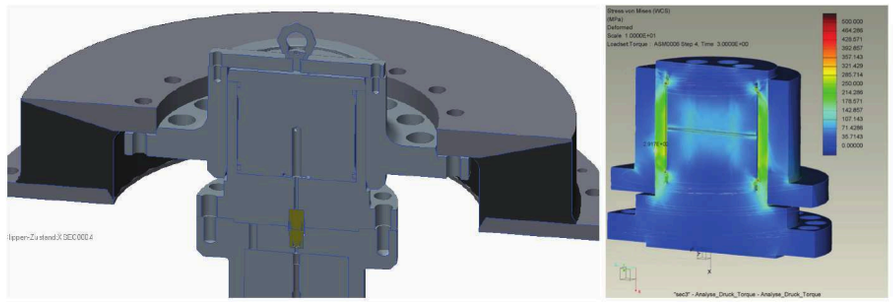

Figure 13: Clamping with FEM-Result

The following conditions have been used for the calculations:

- material: 42CrMo4
- max. allowable von Mises stress: 300 N/mm^2
- max. clamping pressure 700 bar
- tolerance between adapter and hub: H6-f6
- friction coefficient: 0.1

3.5 Test rig design

All three test stations are placed radially around a central column. This is also the housing for the hydraulic aggregate and the electrical cabinets. The test stations have transparent protection covers, which can be moved down and up for assembly and disassembly. Although the transparent covers are open at the top, they were designed to be at such a height that no one can access the test item during testing.

Figure 14: View of the test rig

The frame is made from welded steel profiles and all the doors and cover panels are equipped with sound insulation material to limit the noise emittance.

Figure 15 shows the steel contruction of the test rig.

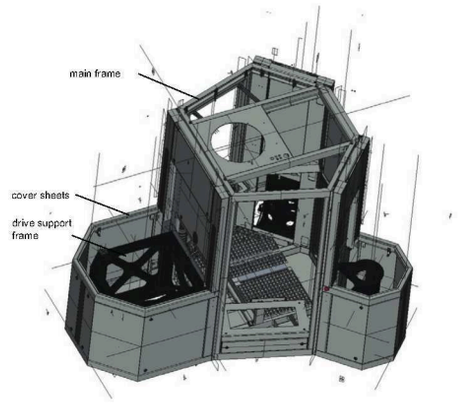

Figure 15: Steel frame

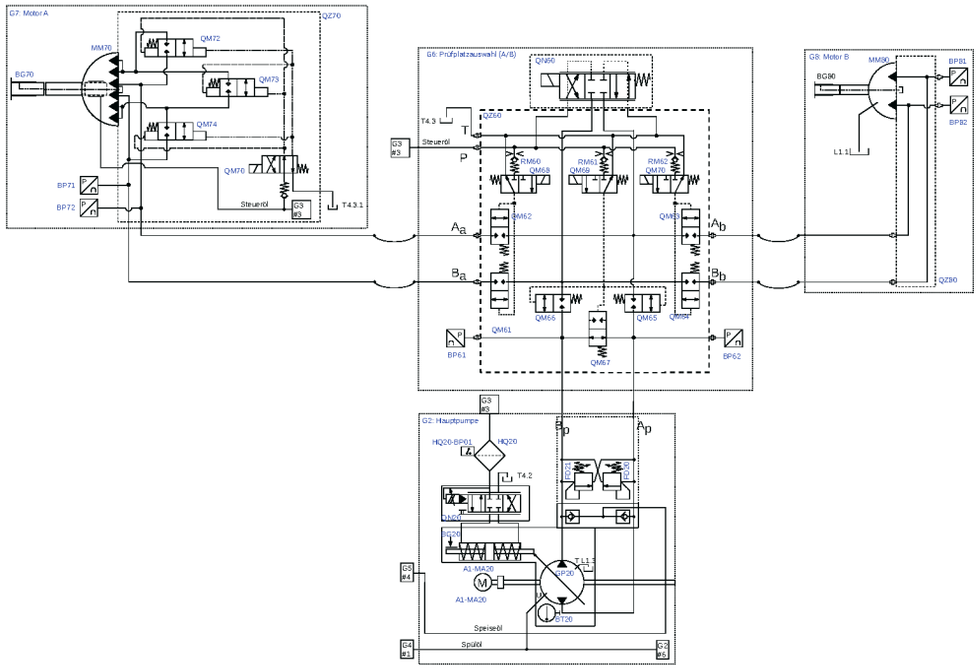

Figure 16: Main hydraulic circuit for station A/B

With the switching block (G6) the main pump can be connected to either motor A or B, which can only be operated alternately. This block also has a control valve for flushing the closed circuit. The variable displacement pump is controlled by a high flow servo valve which allows operation up to a frequency of 10 Hz.

Of course the hydraulic aggregate also has an additional feed oil supply circuit, a control oil circuit as well as a filter and cooling circuit. Details may not be addressed in the scope of this paper. Also, the hydraulic supply of the third motor for the small test station is not shown because this was realized conventionally as a servo-hydraulic axis.

3.6 Test evaluation

The base for the analysis is the time series of torque and angle as shown in figure 4. For evaluation the steady state at 10 Hz excitation is used.

Three different algorithms have been investigated for calculation of the coupling characteristics.

The **correlation method** is a quick and easy method to implement in order to calculate the frequency response for harmonically excited systems. This method is the best choice especially if only discrete frequencies are analyzed.

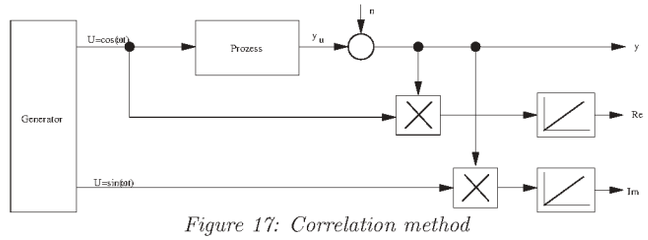

Figure 17: Correlation method

A stable, linear and time invariant system is excitated with a harmonic input signal.

$$u(t) = U \cdot cos(\omega \cdot t) \tag{5}$$

After a settling period the system output is also harmonic.

$$y_u(t) = Y_u \cdot cos(\omega \cdot t + \varphi) \tag{6}$$

Amplitude Y_u and phase shift φ can be picked directly from the frequency response

$$|G(j\omega)| = \frac{Y_u}{U} = \sqrt{Re^2 \cdot [G(j\omega)] + Im^2 \cdot [G(j\omega)]} \tag{7}$$

$$\varphi = arctan\left[\frac{Im[G(j\omega)]}{Re[G(j\omega)]}\right] \tag{8}$$

If the frequency response is calculated from torque to angle, the result for stiffness and damping are:

$$C = G(j\omega)\frac{1}{\sqrt{1+(\omega\varphi)^2}} \tag{9}$$

$$d = 2\pi\left[\frac{Im[G(j\omega)]}{Re[G(j\omega)]}\right] \tag{10}$$

To limit measurement errors it is necessary to integrate over a period of more than 10 cycles.

Another advantage of the correlation method is that it can be evaluated while the test is running. New results for stiffness and damping can be updated and displayed online.

With the **integration method** the area of the ellipse is geometrically integrated.

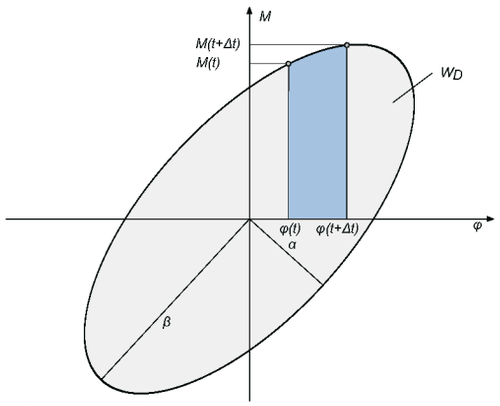

Figure 18: Numeric integration of the ellipse area

$$W_D = \oint M d\varphi \tag{11}$$

Elastic energy W (see figure: 3) can be calculated from the stiffness C, which can be evaluated via linear regression from the torque and angle reading.

In a third procedure a direct **approximation** of the ellipse is made via a regression method /4/. This procedure is well known and used in software-supported pattern recognition.

A comparison of all three methods can be seen in figure 19.

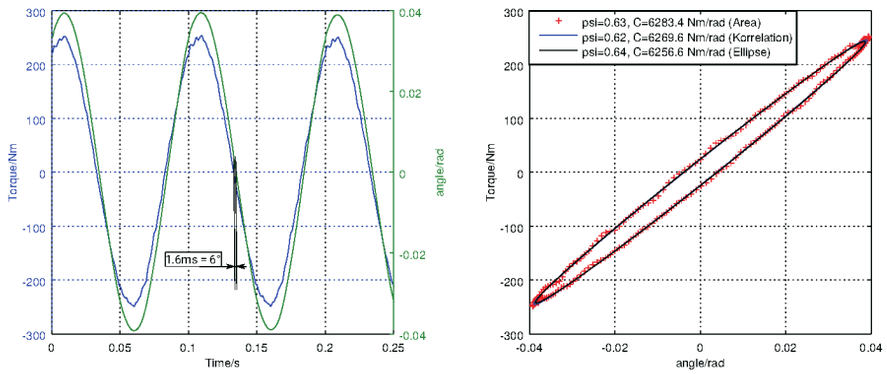

Figure 19: Comparison of three evaluation methods for stiffness and damping

All three methods evaluate the same results with linear material properties. This is as expected. There are differences if nonlinear material behaviour or real world influences of the test rig are present, resulting in degenerated ellipses. The maximum deviation from one another is about 10%. In accordance with the standard (DIN 740), the integration method is finally implemented into the test rig software.

3.6.1 Signal acquisition

Common coupling materials have damping properties in the range of d = 0.65 – 1.15. This results in a phase shift between torque and angle of about: 5.9° – 10.4° at a frequency of 10 Hz. Subsequently, this results in a time shift of 1.6 ms – 2.9 ms between torque and angle.

If the damping calculation is expected to be accurate within an error of 5%, the maximum allowed jitter or time shift between the signals must be smaller than 80 μs.

EtherLab /5/ is used as the automation system. The real time Ethernet: *EtherCAT* has the DC feature (distributed clocks), which can ensure that the jitter between individual samples of a channel, as well as between the channels themselves, is better than 1 μs. The angle signal is determined by a sin/cos encoder and the torque is measured via a signal amplifier with integrated A/D converter.

Both acquisition systems have unknown time shifts in the signal path, which is in the same dimensions than the allowed range. The actual time difference had to be determined by an experimental setup and is evaluated to 110 μs.

4 Summary

This paper presents a dynamic High-Torque Test Stand with hydrostatic drive technology used for production-related testing of elastomeric couplings. Aside from the properties of the test specimen, the hydraulic concept, detailed solutions, such as a torque sensor with end stops, a hydraulically operated clamping system, as well as the evaluation of the obtained measurement results are being addressed.

The test rig has been in operation, ensuring quality products, since April 2017.

References

[1] Murrenhoff, H. *Umdruck zur Vorlesung Servohydraulik*, RWTH Aachen, Germany 2012

[2] Betten Josef, *Zur Ermittlung der mechanischen Hysterese rheologischer Körper*, Zeitschrift für Naturforschung 27 a, Seite 718f., 1972

[3] Becker Markus, *Beanspruchungsgerechte Lebensdauerdimensionierung von dynamisch auf Drehschub belasteten Elastomerkupplungen*, 2006

[4] Radim Halíř, Jan Flusser, *Numerically stable direct Least Squares Fitting of Ellipses*, WSCG'98 Conf. Proc., Feb. 1998.

[5] Ingenieurgemeinschaft IgH, *EtherLab*, `www.etherlab.org`, 2006–2017